# Understanding the Facile Photooxidation of $Ru(bpy)_3^{2+}$ in Strongly Acidic Aqueous Solution Containing Dissolved Oxygen

**Amitava Das,[†] Vishwas Joshi,[‡] Dilip Kotkar,[‡] Vinit S. Pathak,[‡] V. Swayambunathan,[‡] Prashant V. Kamat,*[,§] and Pushpito K. Ghosh*[,†,||]**

*Central Salt & Marine Chemicals Research Institute, G B Road, Bhavnagar 364002, Gujarat, India, ICI India Research & Technology Center, Thane-Belapur Road, Thane 400601, India, and Radiation Laboratory, University of Notre Dame, Notre Dame, Indiana*

*Received: October 27, 2000; In Final Form: May 9, 2001*

The previously observed facile photooxidation of $Ru(bpy)_3^{2+}$ to $Ru(bpy)_3^{3+}$ in oxygenated solutions of 9 M $H_2SO_4$ (Kotkar, D; Joshi, V.; Ghosh, P. K. *Chem. Commun*. **1987**, 4; Indian Patent No. 164358 (1989)) is further studied. A similar phenomenon was observed with $Ru(phen)_3^{2+}$ but not with $Ru(bpy)_2[bpy\text{-}(CO_2H)_2]^{2+}$. The reaction is strongly dependent on acid concentration, with a sharp change in the region of 2−7 M $H_2SO_4$. The quantum yield of $Ru(bpy)_3^{3+}$ formation in 9 M $H_2SO_4$ is close to the quantum yield of steady-state luminescence quenching by $O_2$. Photooxidation is accompanied by near-stoichiometric formation of $H_2O_2$ as reduced product. Chromatographic, spectroscopic, electrochemical and optical rotation studies reveal that $Ru(bpy)_3^{2+}$ survives the strongly acidic environment with little evidence of either any change in coordination sphere or ligand degradation, even after repeated cycles of photolytic oxidation followed by electrolytic reduction. The high quantum yield and selectivity of the reaction is ascribed to (i) predominance of the electron transfer quenching pathway over all others and (ii) highly efficient trapping of $O_2^{\bullet-}$ by $H^+$ followed by rapid disproportionation to $H_2O_2$ and $O_2$. These are likely on account of the high ionic strength of the medium which favors the required shifts in the potentials of the $O_2/O_2^{\bullet-}$ and $O_2/H_2O_2$ couples. Upon storage of the photooxidized Ru(III) solution in dark, partial recovery of $Ru(bpy)_3^{2+}$ occurs gradually. Studies with the electrooxidized complex over a range of acid concentrations indicate that $Ru(bpy)_3^{2+}$ is regenerated by reaction of $Ru(bpy)_3^{3+}$ with $H_2O_2$. The reaction is promoted by increasing concentrations of $[H_2O_2]$ and inhibited by $[O_2]$ and $[H^+]$. The fraction of Ru(III) remaining after the reverse reaction is allowed to plateau in solutions of varying acid concentrations follows a similar trend to that found after attainment of steady state in the photooxidation reaction, although in all cases the forward reaction produces more Ru(III) than what remains in the reverse reaction. These observations are consistent with the following equation $2Ru(bpy)_3^{2+} + O_2 + 2H^+ \rightarrow (h\nu)/\leftarrow (\text{dark})\ 2Ru(bpy)_3^{3+} + H_2O_2$ for which the equilibrium constant has been computed. Light helps overcome the activation barrier of the forward reaction by driving it via $*Ru(bpy)_3^{2+}$, and to the extent that the photooxidation is driven past the equilibrium, there is conversion of light energy in the form of long-lived chemical products. Spectroscopic evidence rules out any significant shift in the redox potential of $Ru(bpy)_3^{3+/2+}$, suggesting thereby that $H_2O_2$ is much more stable in the more strongly acidic medium and less capable of reducing $Ru(bpy)_3^{3+}$ unlike at higher pH.

## Introduction

Photoinduced charge separation involving metal complexes in solution is a widely studied field of research in view of its fundamental importance and potential application for conversion of light energy into chemical energy.[1] Several alternative approaches for solar energy conversion have also been reported.[2] A principal factor that can limit the practical utility of photoredox reactions—more so in solution—is the deleterious back electron transfer within the geminate pair, as shown in eq 1c, where D and A represent donor and acceptor species.[1,3,4]

$$D \xrightarrow{h\nu} D^* \quad (1a)$$

$$D^* + A \rightarrow [D^+ \cdots A^-] \quad (1b)$$

$$[D^+ \cdots A^-] \rightarrow D + A \quad (1c)$$

The photochemistry of $Ru(bpy)_3^{2+}$ (bpy = 2,2′-bipyridine) and related complexes have been at the center stage for many years,[3−5] owing to their unique combination of attractive properties such as high thermal and photochemical stability, strong absorption in the visible region ($\epsilon = 1.4 \times 10^4\ M^{-1}\ cm^{-1}$ for $Ru(bpy)_3^{2+}$ at 450 nm), moderately long-lived ($\sim 0.6\ \mu s$) triplet excited state generated through intersystem crossing, and ability to undergo both reductive and oxidative electron-transfer processes.[3] Indeed, $Ru(bpy)_3^{2+}$ has been utilized in numerous schemes for solar energy conversion.[2e,3−5] Some success has

[†] Central Salt & Marine Chemicals Research Institute.
[‡] ICI India Research & Technology Center.
[§] Radiation Laboratory.
[||] E-mail: salt@csir.res.in.

10.1021/jp0039924 CCC: $20.00 
Published on Web 06/23/2001

been achieved in slowing down the back reaction in interfacial systems,[4−6] and also through judicious selection of reactions which fall within the Marcus "inverted region",[7] but the need for sacrificial agents remains, especially to realize high quantum yields.[8] An attractive scheme for the splitting of water employing $Ru(bpy)_3^{2+}$ as photocatalyst is depicted in eqs 2 and 3. Such a scheme is thermodynamically feasible and

$$*Ru(bpy)_3^{2+} + H^+ \rightarrow [Ru(bpy)_3^{3+} \cdots H] \rightarrow Ru(bpy)_3^{3+} + {}^1/_2H_2 \quad (2)$$

$$Ru(bpy)_3^{3+} + {}^1/_2H_2O \rightarrow Ru(bpy)_3^{2+} + {}^1/_4O_2 + H^+ \quad (3)$$

represents an uphill conversion of light energy into useful chemical energy ($\Delta G$ for eqs 2 and 3 = −0.44 eV and −0.45 eV, respectively, at pH 7, while $\Delta G$ for the overall water splitting reaction, i.e., ${}^1/_2H_2O \rightarrow {}^1/_2H_2 + {}^1/_4O_2$, is 1.23 eV).[3] Indeed, the half-cell reactions have been studied successfully by numerous investigators but the overall goal of water splitting has remained elusive because of the multielectron processes involved, unfavorable energetics of intermediates, and mismatch of the reaction rates within the two half-cells.[9−13] Thus, even if the geminate pair in eq 2 were to form, the back electron process would be inevitable due to the absence of stabilization of the transient hydrogen radical and the slowness of reaction 3,which proceeds in the millisecond-to-second time scale even in the presence of catalysts such as cobaltous ion and oxides of ruthenium and iridium.[3,11−15]

While most of the above work with $Ru(bpy)_3^{2+}$ has been carried out under anaerobic conditions, several laboratories, including ours, have been interested in investigating the photochemistry of $*Ru(bpy)_3^{2+}$ in the presence of oxygen. Oxygen is among several molecules which exhibit high efficiency toward quenching of $*Ru(bpy)_3^{2+}$ in aqueous solution ($k_q = 3.3 \times 10^9\ M^{-1}\ s^{-1}$).[3,16] Much of this work has focused on the issue of charge transfer (CT) vs energy transfer (ET) in this system (eqs 4 and 5).[16−18] Both processes are energetically possible ($\Delta G^o_{CT} = -0.72$ eV; $\Delta G^o_{ET} = -1.17$ eV in $H_2O$ at pH 7.0).[3,16] Lin and Sutin were the first to suggest that quenching occurs via the electron-transfer pathway,[16e] while Winterle et al. demonstrated that photolysis of a solution containing $Ru(bpy)_3^{2+}$, $O_2$, and Fe(II) in acidic solutions leads to formation of Fe(III), which presumably involves such an electron-transfer pathway.[17] Miller et al. proposed that the back electron-transfer process (eq 6) yields singlet oxygen ($^1\Delta_g$),[16d] although this possibility was subsequently discounted by Mulazzani et al.[18a]

$$*Ru(bpy)_3^{2+} + O_2 \rightarrow Ru(bpy)_3^{3+} + O_2^{\bullet -} \quad (4)$$

$$*Ru(bpy)_3^{2+} + O_2 \rightarrow Ru(bpy)_3^{2+} + O_2\ (^1\Delta_g) \quad (5)$$

$$[Ru(bpy)_3^{3+} \cdots O_2^{\bullet -}] \rightarrow Ru(bpy)_3^{2+} + O_2\ (^1\Delta_g) \quad (6)$$

Instead, they proposed that singlet oxygen is formed via direct energy transfer (eq 5). As indicated above, energy transfer is thermodynamically the preferred pathway at pH 7.

In the course of our studies with optically active $Ru(bpy)_3^{2+}$, which necessitated handling of the complex in strongly acidic aqueous medium,[19−21] it was observed that the color of the solution readily converts from orange-yellow to green when left unattended on the laboratory bench. Control experiments established the role of light and oxygen in this process. These observations and some preliminary conclusions were reported by us previously,[22] and similar observations were reported more recently by Zhang and Rodgers.[23] Clearly, eq 4 is implicated and the back reaction of eq 6 is efficiently suppressed. Herein we report our further investigations of the reaction stoichiometry, thermodynamics, and mechanistic pathway.

## Experimental Section

**Reagents.** $Ru(bpy)_3Cl_2 \cdot 2H_2O$ and other Ru(II) derivatives were synthesized following published procedure.[20,24] Enantiomers of $Ru(bpy)_3^{2+}$ were resolved by the method described previously.[19] $Ru(bpy)_3^{3+}$ was prepared either through electrochemical oxidation or by chemical oxidation with $PbO_2$.[12] Methyl viologen (as dichloro salt) was procured from Aldrich and used as received. All other reagents used were of reagent grade, and doubly distilled water was used throughout. The strength of the $H_2O_2$ solution was determined by titrimetric method using freshly prepared standard $KMnO_4$ solution.

**Instrumentation.** UV−vis spectra were recorded on a Pye-unicam model SP8−100 or Shimadzu UV-3101PC spectrophotometer and steady-state luminescence measurements were conducted on a Perkin-Elmer LS-50B spectrofluorimeter. Optical rotation values were measured at the sodium D line using a JASCO DIP 140 digital polarimeter. HPLC studies of photolyzed and control solutions of $Ru(bpy)_3^{2+}$ were conducted on a model 6000A Water's instrument, with model 481 solvent delivery system, UV−vis detector, and model 730 data module, using a $C_{18}$ column and the method described.[12] $^1H$ NMR spectra were recorded on a Bruker-80 spectrometer, elemental analysis was performed on a Carlo Erba elemental analyzer (model 1106), and IR spectra were recorded on a Perkin-Elmer instrument. Cyclic voltammograms were recorded on a CH660A instrument, using a three electrodes cell assembly comprising a glassy carbon working electrode, a Pt counter electrode and Ag−AgCl reference electrode, while bulk electrolysis was carried out using a cylindrical Pt-mesh working electrode. Viscosity measurements of acid solutions were made using an Ostwald viscometer.

**Photocurrent Measurements.** Photocurrents were recorded on a multimeter fitted to Pt gauze electrodes ($\sim$ 5 $cm^2$ total area of each electrode) in the two half-cells. Fine glass frits separated the half-cells, and a buffer compartment (containing 4.5 M $H_2SO_4$) further ensured minimum contamination of the half-cells.

**Lifetime and Transient Absorption Measurements.** Nanosecond laser flash photolysis experiments were performed using 532 nm (second harmonic) laser pulse ($\sim$6 ns laser width) from a Quanta Ray model CDR-1 Nd:YAG laser system for excitation in the experiments of Figures 7 and 8.[25a,b] The laser output was suitably attenuated to about 20 mJ/pulse and defocused to minimize the multiphoton process. The experiments were performed in a rectangular quartz cell of 6 mm path length with a right angle configuration between the direction of laser excitation and analyzing light. The photomultiplier output was digitized with a Tektronix 7912 AD programmable digitizer. A typical experiment consisted of a series of 5 replicate shots/single measurement. The average signal was processed with an LSI-11 micro processor. A Spectra Physics model PR0230 laser system (355 nm, 10 ns pulse width, 40 mJ/pulse) was used in the experiment of Figure 9. The average signal was processed with a Le Croy digitizer.[25c] Luminescence lifetimes of $*Ru(bpy)_3^{2+}$ were also measured on the above instrument using 355 nm laser pulse excitation and 650 nm detection.

**Quantum Yield Measurements.** Quantum yield of the photooxidation reaction was estimated through comparative studies with the EDTA/$Ru(bpy)_3^{2+}$/$MV^{2+}$ ($MV^{2+}$ = methyl viologen) system, for which the absolute quantum yield for

$MV^{+\bullet}$ formation via eqs 7−9 has been reported ($\varphi \sim 0.30$ for $[Ru(bpy)_3^{2+}] = 0.04$ mM, $[MV^{2+}] = 2.0$ mM, [EDTA] = 30 mM; pH ~ 5.0).[1j]

$$Ru(bpy)_3^{2+} \xrightarrow{h\nu} {}^*Ru(bpy)_3^{2+} \quad (7)$$

$${}^*Ru(bpy)_3^{2+} + EDTA \rightarrow Ru(bpy)_3^{+} + \text{decomposed product of EDTA} \quad (8)$$

$$Ru(bpy)_3^{+} + MV^{2+} \rightarrow Ru(bpy)_3^{2+} + MV^{+\bullet} \quad (9)$$

The experiments were conveniently carried out in cuvettes suitably adapted to allow purging with nitrogen/oxygen gas and which could be placed directly in the absorption spectrophotometer for monitoring the extent of reaction (change of $Ru(bpy)_3^{2+}$ concentration in the case of the photooxidation reaction and formation of the blue $MV^{+\bullet}$ radical ion in the case of the sacrificial system). The $Ru(bpy)_3^{2+}$ concentrations (0.04 mM) in both experiments were maintained the same and care was taken to ensure that both cuvettes "see" the same intensity of sunlight. The duration of illumination was maintained such that < 30% of the $Ru(bpy)_3^{2+}$ is converted to $Ru(bpy)_3^{3+}$ in the photooxidation system. Typically, the exposure time to bright sunlight was 10−15 s. (Saturation effects introduced error in measurement if we extend the photolysis for a longer time.)

**Estimation of $H_2O_2$ Produced in the Photooxidation Reaction.** Experiments were conducted in a pear-shaped flask fitted with a specially designed curved hollow stopper (in which $MnO_2$ powder is placed to decompose $H_2O_2$ into $O_2$) and a sidearm containing a stopcock capped at the end with a leakproof rubber septum. A thin polypropylene tubing was guided through this septum into the flask bottom and was employed for purging the solution. A narrow gauge needle inserted into the septum served as gas outlet. The volume of the flask, inclusive of the volume of the sidearm and hollow stopper, was ca. 220 mL and a precise volume of 212 mL of solution was taken in the flask each time so as to leave a free space of ca. 8 mL. In the first set of experiments, the evolution of oxygen gas generated from decomposition of $H_2O_2$ (in 9 M $H_2SO_4$) was studied in the concentration range of 0.2−0.8 mM. In the second set of experiments, oxygen evolution following addition of $MnO_2$ powder into the deaerated photolyzed solutions of $Ru(bpy)_3^{2+}$ was studied, in the Ru(II) concentration range, 0.4−1.6 mM. Further details of the experiments are as follows:

*$H_2O_2$ in 9 M $H_2SO_4$.* Two hundred twelve milliliters of a 0.2 mM solution was taken in the flask equipped with a magnetic stirrer and the stopper containing excess of solid $MnO_2$ was carefully placed on the flask, taking care that the powder did not come in contact with the solution. The entire assembly was ensured to be leak proof. The solution was purged with helium gas under stirring to eliminate all traces of $O_2$. The purge tube and outlet were withdrawn from the flask and the stopcock closed. The $MnO_2$ powder was then gently tapped into the flask and generation of gas bubbles could be observed. The solution was allowed to stir for 2 h at room temperature, after which a 1 mL sample of the gas in the free space was taken in an airtight gas syringe and injected into the GC (HP 5890) instrument fitted with a TCD detector and a 6′ × 1/8″ molecular sieve column (5 Å) maintained at 50 °C. The sample injection volume was 1 mL. The injector, column, and detector temperatures were 70, 50, and 100 °C, respectively, and the carrier gas pressure 20 psi. The area of the $O_2$ peak was corrected for contamination from trace air (this was assumed to be one-quarter of the GC area for the nitrogen peak). The same methodology was followed for other $H_2O_2$ concentrations investigated.

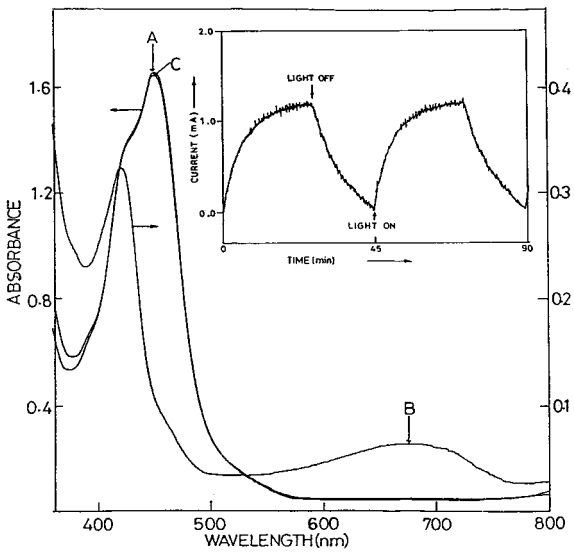


**Figure 1.** Absorption spectral changes for a solution of $1.2 \times 10^{-4}$ M $Ru(bpy)_3^{2+}$ in 9 M $H_2SO_4$: (a) freshly prepared $O_2$-saturated solution in dark, (b) after exposure to bright sunlight, and (c) when an equivalent amount of ferrous ammonium sulfate was added to the solution in (b) above. Inset shows the current vs time plot for $1.0 \times 10^{-3}$ M $Ru(bpy)_3^{2+}$ in $O_2$-saturated 9 M $H_2SO_4$ with sequential photooxidation and electrolytic reduction in dark.

*Photolyzed Solutions of $Ru(bpy)_3^{2+}$ in 9 M $H_2SO_4$.* Two hundred twelve milliliters of 0.4 mM $Ru(bpy)_3^{2+}$ in 9 M $H_2SO_4$ was used instead of 0.2 mM $H_2O_2$ in 9 M $H_2SO_4$ and, as before, the hollow stopper containing excess $MnO_2$ powder was carefully placed in the flask and the solution purged with oxygen for 1 h under stirring, while avoiding exposure of the flask to light. The solution was then irradiated until complete oxidation of Ru(II) was evident. Thereafter, the solution was purged with helium and the procedure described above for 0.2 mM $H_2O_2$ in 9 M $H_2SO_4$ was repeated. The same methodology was followed for other $Ru(bpy)_3^{2+}$ concentrations investigated.

## Results

A 0.05−0.50 mM solution of $Ru(bpy)_3^{2+}$ in $O_2$-saturated acidic solution [9 M $H_2SO_4$] changes color rapidly from yellowish orange to green, when the glass test tube (ca. 1" diameter) containing the solution is exposed to sunlight (Figure 1). Similar observations were made with $Ru(phen)_3^{2+}$ (phen = 1,10-phenanthroline) whereas analogous changes were not found with $Ru(bpy)_2(4,4'\text{-dicarboxy-}2,2'\text{-bpy})^{2+}$. The observation described above was also made with $Ru(bpy)_3^{2+}$ dissolved in 17.4 M $HClO_4$ while there was only a partial change in color in 12 M HCl. Complete reaction was found to be increasingly more difficult at higher concentrations of $Ru(bpy)_3^{2+}$. The absorption spectrum of the green solution obtained from $Ru(bpy)_3^{2+}$ matches exactly the spectrum of $Ru(bpy)_3^{3+}$ generated either by bulk electrolysis or by chemical oxidation with $PbO_2$.[12] Addition of an equimolar amount of ferrous ammonium sulfate restores instantly the original spectrum of the solution. Bulk electrolytic reduction of photooxidized solution (experiment conducted with 9.2 mL of 4.2 mM $Ru(bpy)_3^{2+}$) also yields similar results and the required number of coulombs ($Q_{obs}$ = 3.49 coulombs vs $Q_{calc}$ = 3.58 coulombs) matches that for 1-electron reduction. Further, the oxidation−reduction cycle can be repeated several times without any noticeable irreversibility (see inset in Figure 1).

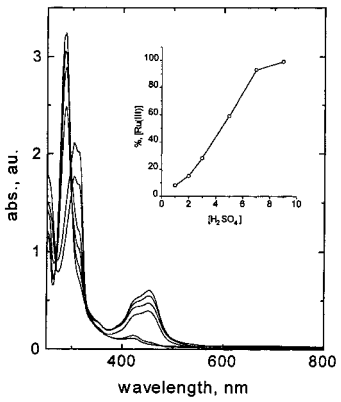


**Figure 2.** Absorption spectra of $1.6 \times 10^{-4}$ M $Ru(bpy)_3^{2+}$ in 1, 2, 3, 5, 7, and 9 M $H_2SO_4$ when exposed to sunlight in the presence of $O_2$. Inset shows the steady-state concentration of Ru(III) for the same solutions.

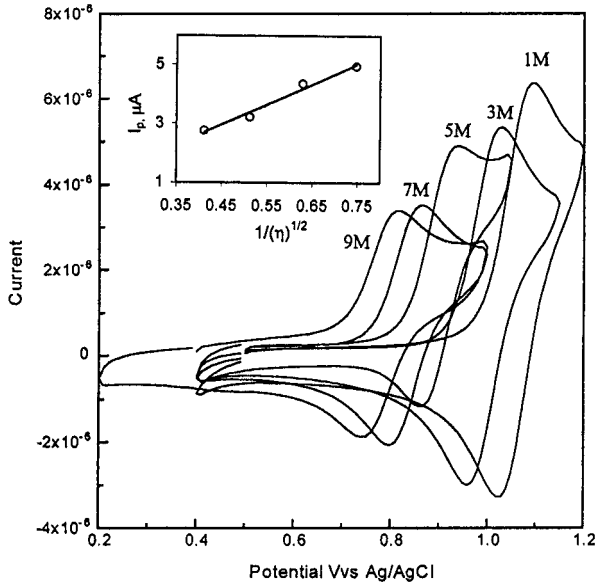


**Figure 3.** Cyclic voltammograms of $2.4 \times 10^{-3}$ M $Ru(bpy)_3Cl_2$ in $N_2$-purged solutions of 1, 3, 5, 7, and 9 M $H_2SO_4$. Voltammograms were recorded at 100 mV $s^{-1}$ in the dark employing a glassy carbon working electrode, a Pt wire counter electrode and Ag/AgCl reference. The inset shows the plot of $i_p$ vs $(1/\eta)^{1/2}$, using the $\eta$ values obtained at different acid concentrations.

Studies were also conducted on continuous illumination of the solution in a divided cell, where the other compartment contained $I^-$ or $Fe^{2+}$ as reductant, and the electrodes of the two compartments were connected via an external circuit. Beyond a turnover number of 10, complete photooxidation of $Ru(bpy)_3^{2+}$ became increasingly difficult. The same system in the absence of $O_2$ (removed by bubbling Ar through the solution), or when kept in the dark for 72 h, or when the acid concentration is reduced below 1 M $H_2SO_4$ does not show any change in absorption spectrum, although at intermediate acid concentrations partial oxidation of Ru(II) is observed spectrophotometrically (Figure 2). There is also no change in the optical rotation value of a $\Delta$-$(-)_D$-$Ru(bpy)_3^{2+}$ solution (in 9 M $H_2SO_4$) which is stored in the dark for up to 7 days.[26]

Cyclic voltammograms of the Ru(II) solutions as a function of acidity show a progressive decrease in the reduction potential and peak current ($i_p$) with acid concentration, as shown in Figure 3. The inset shows the plot of $i_p$ vs $\eta^{-1/2}$, where $\eta$ is the viscosity of the medium. Changes in the reduction potential and steady-state photocurrent density with acid concentration (measured

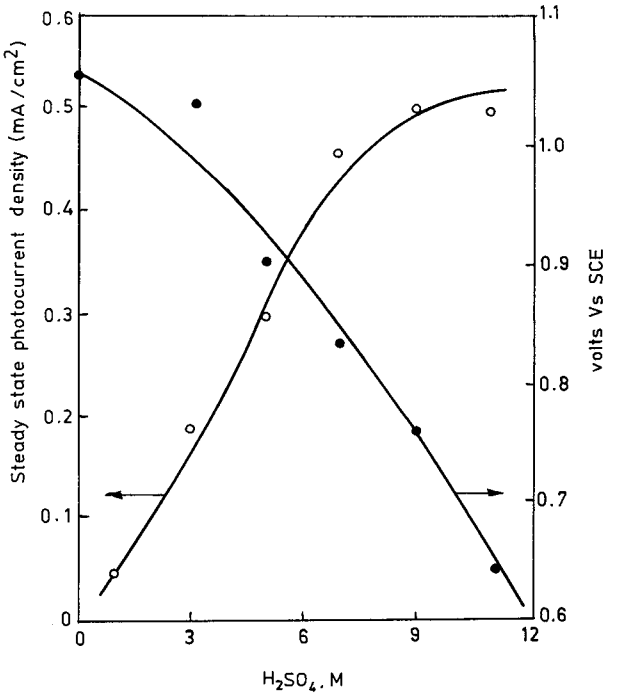


**Figure 4.** Plots of steady-state photocurrent and $E°$ (by cyclic voltammetry) as a function of $[H_2SO_4]$. Steady-state photocurrent measurements were performed using a divided cell as described in the Experimental Section, a constant illumination source, and with $1.6 \times 10^{-4}$ M $Ru(bpy)_3^{2+}$ in the cathodic compartment and 1 M $Fe^{2+}$ (in 1 M $H_2SO_4$) in the anodic compartment.

keeping all other variables constant) are plotted in Figure 4. As can be seen from Figure 4, a photocurrent density of ~0.5 mA $cm^{-2}$ could be sustained with the highest concentration of acid studied.

Spectral (UV−vis, $^1H$ NMR and IR) data, liquid chromatograms, and cyclic voltammograms of a freshly prepared $Ru(bpy)_3^{2+}$ solution and a solution subjected to five complete cycles of photooxidation followed by electrolytic reduction in a divided cell were found to be almost identical (Supporting Information, Figure 1). Elemental analysis and optical rotation data were also obtained on the above samples and the results are comparable.[27] The reduced product formed along with $Ru(bpy)_3^{3+}$ in the photochemical reaction was investigated. As shown in Figure 5, $H_2O_2$ is produced in near stoichiometric yields at low concentrations of Ru(II) while deviations are observed at higher concentrations.

The luminescence lifetime ($\tau_0$) values were similar (~0.5 $\mu$s) for $Ru(bpy)_3^{2+}$ dissolved in degassed solutions of varying acid concentration whereas the lifetimes ($\tau$) measured in $O_2$-saturated solutions showed a systematic change with increasing acidity (Table 1). Steady-state luminescence spectra of $5.12 \times 10^{-5}$ M $Ru(bpy)_3^{2+}$ in water and in 9 M $H_2SO_4$ recorded under $O_2$-saturated and $O_2$-free environments are shown in Figure 6. The peak luminescence intensity in $O_2$-saturated acidic solution is quenched by ca. 30% whereas in water the extent of quenching is ca. 70%. There was no detectable difference in the absorption spectra of $Ru(bpy)_3^{2+}$ recorded in water and in 9 M $H_2SO_4$ (Supporting Information; Figure 2). The quantum yield measurements of Ru(III) formation in $O_2$-saturated 9 M $H_2SO_4$ yielded values in the range of 0.25−0.28. Transient absorption spectral measurements were also performed on this system. As can be seen from the difference absorption spectrum in Figure 7 recorded immediately after a laser flash, 395 nm is the isosbestic point for the ground- and excited-state forms of the

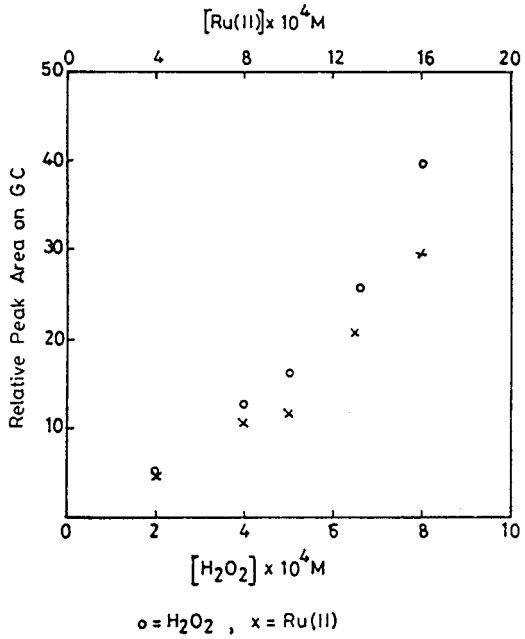


**Figure 5.** GC area count vs concentration of $H_2O_2$/$Ru(bpy)_3^{2+}$ for $O_2$ generated by addition of $MnO_2$ into solutions of $H_2O_2$ in 9 M $H_2SO_4$ (o) and in photolyzed solutions of $Ru(bpy)_3^{2+}$ in 9 M $H_2SO_4$ (x).

Ru(II) complex. Figure 8 shows the time-resolved absorbance changes recorded at the monitoring wavelengths of 395 and 650 nm, respectively, following pulsed laser excitation of Ru(II) in $O_2$-saturated 9 M $H_2SO_4$. The traces show irreversible bleaching of absorbance at 395 nm and absorption gain at 650 nm. Similar studies were performed over a range of acid concentrations and the traces obtained at the monitoring wavelength of 395 nm are shown in Figure 9. The extent of bleaching varies with acid concentration and the process is irreversible up to 160 $\mu$s, which is the longest time scale over which the transient measurements could be performed. Unlike with $Ru(bpy)_3^{2+}$, no bleaching was observed with $Ru(bpy)_2(4,4'\text{-dicarboxy-}2,2'\text{-bpy})^{2+}$ in 9 M $H_2SO_4$. Indeed, the luminescence was not quenched at all by $O_2$ in steady-state experiments.

When the photochemically oxidized ruthenium complex (in 9 M $H_2SO_4$) is stored in dark under ambient aerated conditions, partial reduction to Ru(II) is observed. An identical solution of $Ru(bpy)_3^{2+}$ in 9 M $H_2SO_4$, which is electrochemically oxidized under a blanket of $N_2$, undergoes negligible change when stored in the dark under aerated conditions for 4 h. However, upon addition of a stoichiometric amount of $H_2O_2$, the same extent of reduction is observed as found for the photochemically oxidized complex (Supporting Information; Figure 3). Table 2 provides data on the effect of $[H^+]$ on the maximum observed extent of reduction of Ru(III), keeping other parameters constant, while Figure 10 shows a plot of these data. In 1, 5, and 9 M $H_2SO_4$, the time required for 25% reduction is ca. 0.25, 0.75, and 4 h, respectively. At the lower acid concentrations, further reduction is observed over longer durations. Table 3 provides additional data on the effect of $[O_2]$ and $[H_2O_2]$. As can be seen from Tables 2 and 3 together, the reduction is inhibited by $[O_2]$ and $[H^+]$ but promoted by $[H_2O_2]$.

## Discussion

**Photooxidation.** Figures 1 and 2 indicate that $Ru(bpy)_3^{2+}$ undergoes quantitative 1-electron photoinduced oxidation to $Ru(bpy)_3^{3+}$ (eq 4) in oxygenated solutions, when $[H_2SO_4] \geq 7$ M. Only partial reaction is observed at lower acidities, with a dramatic transition in the $[H_2SO_4]$ range of 2−7 M, as shown in Figure 2. Although our studies have focused on $H_2SO_4$, the choice of acid may not be critical—but its strength is—since quantitative photooxidation could be effected in 17.4 M $HClO_4$ as well. The oxidized complex can be reduced back to $Ru(bpy)_3^{2+}$ quantitatively, either through the addition of reductants such as $Fe^{2+}$ or electrochemically, and the cycle repeated as evident from the inset of Figure 1. The negligible formation of side products in the process is evident from the spectroscopic, electrochemical, and HPLC data together with the elemental analysis results.[27] Optical rotation measurements further support the inertness of the Ru(II) complex toward any form of innersphere substitution reaction under the experimental conditions used and confirm the outersphere nature of the observed photoredox process.[26,27] The clean photooxidation of $Ru(bpy)_3^{2+}$ would necessarily have to be accompanied by the formation of a reduced product, which has now been identified as $H_2O_2$, its yield being close to quantitative for $[Ru(bpy)_3^{2+}] \leq 0.4$ mM (Figure 5). Poor sensitivity might have eluded earlier detection of the species, leading us to speculate that $H_2O$ is possibly formed as the reduced product.[22b] This difficulty was overcome in the present work by maintaining a minimum gas space in the reaction flask (based on Henry's law, $x = p/K$, where $x$ is the mole fraction of $O_2$ in solution, $p$ is the partial pressure of $O_2$ in the gas phase, and $K$ is Henry's constant [$K = 3.30 \times 10^7$ Torr in water]) which yielded a measurable $O_2$ peak in the GC which was duly corrected for background oxygen.

The standard reduction potential of $Ru(bpy)_3^{3+/2+}$ is 1.26 V vs NHE in water and the potential remains unaltered up to 1 M $H_2SO_4$. However, beyond this acid concentration, the peak current and reduction potential decrease dramatically with increased acidity as evident from Figure 3 and Table 4.[28] Concomitantly, the solution viscosity rises with acid concentration. The changes in peak current can be rationalized on the basis of eq 10 ($D_1$ and $D_2$ are the diffusion coefficients in media 1 and 2, respectively, while $\eta_1$ and $\eta_2$ are the corresponding viscosities) and eq 11 ($n$ is the number of electrons involved in the redox process, $A$ is the electrode area, $C_0$ and $D_0$ are the concentration and diffusion coefficient, respectively, of the electroactive species, $\upsilon$ is the scan rate),[29] as can be seen from the inset in Figure 3. The shifts in potential could

$$D_1\eta_1 = D_2\eta_2 \tag{10}$$

$$i_p = 0.4463nFAC_0(nF/RT)^{1/2}\upsilon^{1/2}D_0^{1/2} \tag{11}$$

account for the more facile oxidation at higher acidities but are difficult to rationalize, given the lack of any corresponding changes in the absorption and luminescence spectra as also in the measured optical rotation value of the $\Delta$-$(-)_D$ complex. Quantitatively, the shift observed for $Ru(bpy)_3^{3+/2+}$ is 280 mV for increase in acid concentration from 1 to 9 M, which matches closely with the shift of ca. 290 mV found for the ferrocinium/ferrocene couple (Table 4). This suggests to us that the observed trend is an artifact of unaccounted change in the junction potential. For $Ru(phen)_3^{3+/2+}$ and $Ru(bpy)_2(4,4'\text{-dicarboxy-}2,2'\text{-bpy})^{3+/2+}$, the corresponding shifts are 350 and 200 mV, respectively, indicating that the phen complex, after accounting for junction potential, is more readily oxidizable in strong acid whereas $Ru(bpy)_2(4,4'\text{-dicarboxy-}2,2'\text{-bpy})^{2+}$ becomes even more difficult to oxidize in strong acid than in water. This could explain the inertness of the latter to photooxidation in 9 M $H_2SO_4$.

Results of the luminescence studies (Figure 6) indicate a maximum quantum yield, $\phi$, of 0.30 for the quenching of

**TABLE 1: Lifetime Measurements of *Ru(bpy)$_3^{2+}$ as a Function of Acid Concentration[a]**

| $[H_2SO_4]$ (M) | $\tau_0$ ($N_2$-purged) ($\mu$s) | $\tau$ ($O_2$-purged) ($\mu$s) | $\eta_{rel}$ | $k_D$ | $[\tau_0/\tau]_{obs}$ | $[\tau_0/\tau]_{calc}$[b] |
|---|---|---|---|---|---|---|
| 0 | 0.520 | 0.166 | 1 | $3.30 \times 10^9$ | 3.13 | 3.19 |
| 1 | 0.491 | 0.196 | | | 2.50 | |
| 2 | 0.522 | 0.208 | | | 2.51 | |
| 3 | 0.547 | 0.238 | 1.79 | $1.84 \times 10^9$ | 2.30 | 2.29 |
| 5 | 0.549 | 0.290 | 2.53 | $1.30 \times 10^9$ | 1.89 | 1.91 |
| 7 | 0.531 | 0.354 | 3.82 | $8.64 \times 10^8$ | 1.50 | 1.59 |
| 9 | 0.522 | 0.398 | 5.90 | $5.59 \times 10^8$ | 1.31 | 1.37 |

[a] Solutions containing 0.16 mM Ru(bpy)$_3^{2+}$. [b] $[\tau_0/\tau]_{calc} = 1 + k_D\tau_0[O_2]_{sat}$, with $[O_2]_{sat} = 1.28$ mM for all acid concentrations.

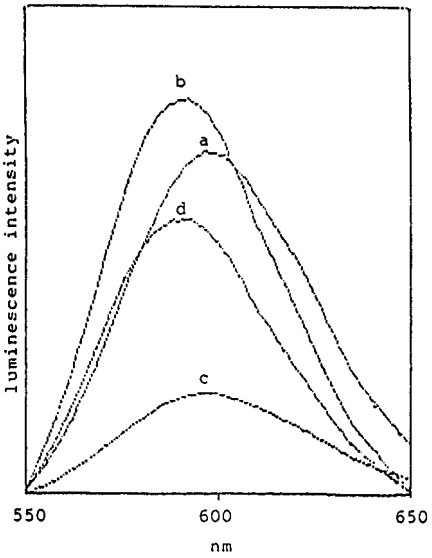


**Figure 6.** Luminescence spectra of $N_2$ purged solutions of $5.12 \times 10^{-5}$ M Ru(bpy)$_3^{2+}$ in (a) water and (b) in 9 M $H_2SO_4$. The corresponding luminescence spectra of the above solutions after purging with $O_2$ are shown in (c) and (d), respectively.

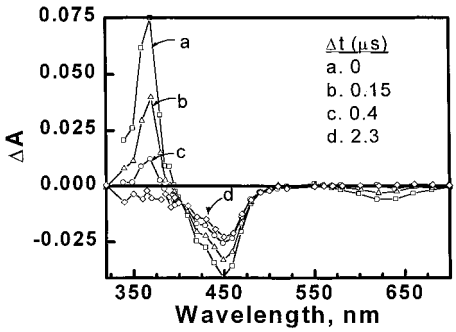


**Figure 7.** Difference absorption spectra of an $O_2$-saturated solution of $2.0 \times 10^{-4}$ M Ru(bpy)$_3^{2+}$ in 9 M $H_2SO_4$ recorded after time intervals of (a) 0 $\mu$s, (b) 0.156 $\mu$s, (c) 0.39 $\mu$s and (d) 2.34 $\mu$s. The excitation wavelength and radiation dose were 532 nm and 15 mJ, respectively. The apparent bleaching in the long wavelength region (~650 nm) is due to luminescence.

*Ru(bpy)$_3^{2+}$ by $O_2$ in $O_2$-saturated 9 M $H_2SO_4$ whereas the value is considerably higher in water ($\phi = 0.70$). The quenching has been reported to be diffusion-controlled in water, with $k_D = 3.3 \times 10^9$ M$^{-1}$ s$^{-1}$.[3,16] On the basis of eqs 10 and 12 ($D_A$ and $D_B$ are the diffusion coefficients of the two reactant species, $\beta$ is the reaction radius and $N_0$ the Avogadro's number),[30] and

$$k_D = 4\pi(D_A + D_B)\beta N_0/1000 \qquad (12)$$

assuming the reaction remains diffusion-controlled in all cases, changes in $k_D$ with acid concentration have been computed and

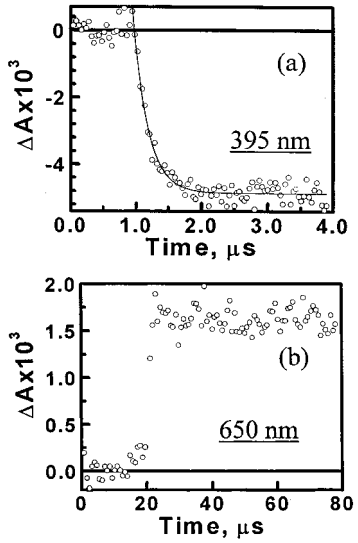


**Figure 8.** Time-resolved absorption spectra of an $O_2$-saturated solution of $2.0 \times 10^{-4}$ M Ru(bpy)$_3^{2+}$ in 9 M $H_2SO_4$ recorded at (a) 395 nm and (b) 650 nm. The plots were recorded employing 532 nm excitation wavelength and dose levels of 21.4 mJ and 81.77 mJ/pulse for (a) and (b), respectively.

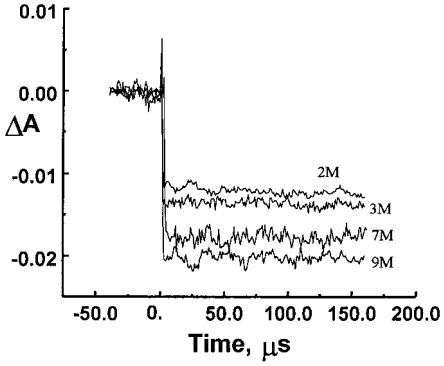


**Figure 9.** Plots of $\Delta A$ vs time for 0.16 mM Ru(bpy)$_3^{2+}$ in $H_2SO_4$ solutions of varying molarity. The excitation and monitoring wavelengths were 355 and 395 nm, respectively, and the dose level was 40 mJ/pulse.

are shown in Table 1. Using eq 13 below,[31] and assuming $[O_2]$ remains constant at all acid concentrations studied ($[O_2] = 1.28$ mM in water at a

$$\tau_0/\tau = 1 + k_D\tau_0[O_2] \qquad (13)$$

partial pressure of 760 Torr and $T = 298$ K),[32] values of $\tau_0/\tau$ have been computed ($[\tau_0/\tau]_{calc}$) and tally closely with the values ($[\tau_0/\tau]_{obs}$) obtained from luminescence lifetime measurements (Table 1). Therefore, $[O_2]_{sat}$ can be taken as 1.28 mM for all calculations pertaining to these solutions and the observed effects can be entirely explained by the changes in $k_D$ as a result of

**TABLE 2: Computation of Molar Equilibrium Constant ($K_c$) for Equation 25 at Different Acid Concentrations[a]**

| $H_2SO_4$ | | | $H^+$, eq[b] | | | | | | | |
|---|---|---|---|---|---|---|---|---|---|---|
| $\rho$, g $mL^{-1}$ | M | m | $[\gamma_{H^+}]_m$[c] | M | $[\gamma_{H^+}]_M$[d] | Ru(III), eq M | Ru(II), eq M | $H_2O_2$, eq M | $O_2$, eq M | $K_c$[e] |
| 1.13 | 2 | 2.14 | 0.93 | 2 | 0.996 | $0.30 \times 10^{-5}$ | $2.70 \times 10^{-5}$ | $0.15 \times 10^{-5}$ | $28.65 \times 10^{-5}$ | $1.63 \times 10^{-5}$ |
| 1.19 | 3 | 3.35 | 1.40 | 3 | 1.563 | $0.46 \times 10^{-5}$ | $2.54 \times 10^{-5}$ | $0.23 \times 10^{-5}$ | $28.73 \times 10^{-5}$ | $1.19 \times 10^{-5}$ |
| 1.30 | 5 | 6.17 | 4.90 | 5 | 6.048 | $1.55 \times 10^{-5}$ | $1.45 \times 10^{-5}$ | $0.78 \times 10^{-5}$ | $29.27 \times 10^{-5}$ | $3.33 \times 10^{-5}$ |
| 1.42 | 7 | 9.54 | 19.00 | 7 | 25.890 | $1.98 \times 10^{-5}$ | $1.02 \times 10^{-5}$ | $1.00 \times 10^{-5}$ | $29.49 \times 10^{-5}$ | $0.39 \times 10^{-5}$ |
| 1.53 | 9 | 13.89 | | 9 | | $2.20 \times 10^{-5}$ | $0.80 \times 10^{-5}$ | $1.10 \times 10^{-5}$ | $29.60 \times 10^{-5}$ | |

[a] Experiments were performed with electrochemically generated $Ru(bpy)_3^{3+}$ (in 9 M $H_2SO_4$) which was subsequently adjusted to yield solutions with the same initial Ru(III) concentration [$3.0 \times 10^{-5}$ M] but with varying acid concentrations. The solutions were air-saturated ([$O_2$] = $3.0 \times 10^{-4}$ M) and kept in the dark for 4 h. During this period, the reduction of Ru(III) to Ru(II) by the medium alone was negligible. [b] $H_2SO_4$ exists as $H^+$ and $HSO_4$- over this range of acid concentration.[39a] [c] Values based on ref 40 and Figure 4 of Supporting Information. [d] Values computed using eq 26. [e] $K_c = [Ru(III)]^2[H_2O_2]/\{[\gamma_{H^+}]_M.[H^+]\}^2[Ru(II)]^2[O_2]$, where the concentrations are those at equilibrium.

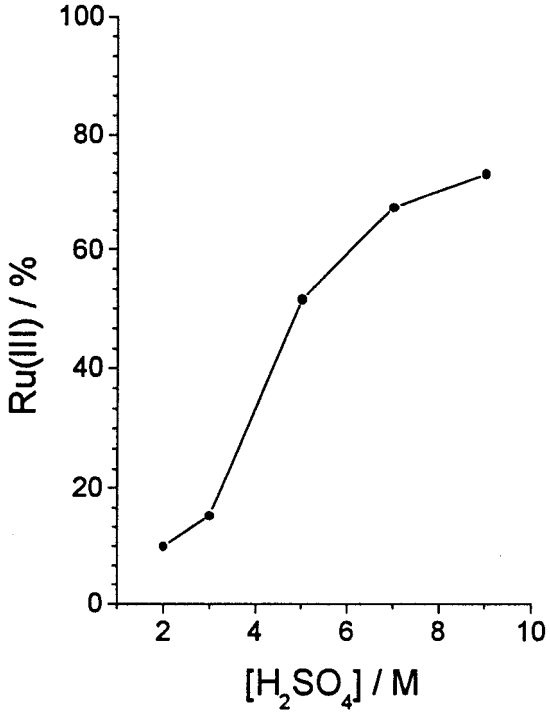


**Figure 10.** Plot of Ru(III) (as % of total Ru) at equilibrium vs [$H_2SO_4$] based on the data of Table 2.

changes in viscosity. Further, using eq 14 below,[31] where $I_0$ and $I$ are the steady-state peak luminescence intensities in $O_2$-free and $O_2$-saturated solutions, the observed differences in luminescence quenching efficiencies in water and in 9 M $H_2SO_4$ (Figure 6) can be nicely accounted for [$I_0/I =$

$$I_0/I = \tau_0/\tau \qquad (14)$$

3.3 in water vs 1.4 in acid; corresponding $\tau_0/\tau$ values are 3.13 and 1.31 (Table 1)].

Alternative schemes may be proposed for the excited-state quenching and subsequent transformations ($O_2$ implies ground-state oxygen molecule). Schemes 1 and 2 pertain to quenching via electron transfer. In the former scheme, $HO_2^\bullet$ disproportionates to produce $H_2O_2$ (eq 20) or oxidizes a second *$Ru(bpy)_3^{2+}$ (eq 18). In the second scheme, $HO_2^\bullet$ oxidizes ground-state $Ru(bpy)_3^{2+}$, i.e., both ground and excited states of the complex are involved in $H_2O_2$ formation. Note that in Scheme 2, the quantum yield would be double that of Scheme 1 and the oxidation of $Ru(bpy)_3^{2+}$ to $Ru(bpy)_3^{3+}$ would occur in two distinct time domains. Scheme 3 depicts deactivation to ground state via formation of an intermediate collision complex,[23] and Scheme 4 represents energy transfer quenching to produce singlet oxygen.

**SCHEME 1**

$$*Ru(bpy)_3^{2+} + O_2 \rightarrow [Ru(bpy)_3^{3+}\cdots O_2^{\bullet -}] \qquad (15)$$

$$[Ru(bpy)_3^{3+}\cdots O_2^{\bullet -}] \rightarrow Ru(bpy)_3^{2+} + O_2\ (\text{or } {}^1O_2) \qquad (16)$$

$$[Ru(bpy)_3^{3+}\cdots O_2^{\bullet -}] + H^+ \rightarrow Ru(bpy)_3^{3+} + HO_2^\bullet \qquad (17)$$

$$*Ru(bpy)_3^{2+} + HO_2^\bullet \rightarrow Ru(bpy)_3^{3+} + HO_2^- \qquad (18)$$

$$HO_2^- + H^+ \rightarrow H_2O_2 \qquad (19)$$

$$2HO_2^\bullet \rightarrow H_2O_2 + O_2 \qquad (20)$$

$$2Ru(bpy)_3^{3+} + H_2O_2 \rightarrow 2Ru(bpy)_3^{2+} + O_2 + 2H^+ \qquad (21)$$

**SCHEME 2**

$$*Ru(bpy)_3^{2+} + O_2 \rightarrow [Ru(bpy)_3^{3+}\cdots O_2^{\bullet -}] \qquad (15)$$

$$[Ru(bpy)_3^{3+}\cdots O_2^{\bullet -}] \rightarrow Ru(bpy)_3^{2+} + O_2\ (\text{or } {}^1O_2) \qquad (16)$$

$$[Ru(bpy)_3^{3+}\cdots O_2^{\bullet -}] + H^+ \rightarrow Ru(bpy)_3^{3+} + HO_2^\bullet \qquad (17)$$

$$Ru(bpy)_3^{2+} + HO_2^\bullet \rightarrow Ru(bpy)_3^{3+} + HO_2^- \qquad (22)$$

$$HO_2^- + H^+ \rightarrow H_2O_2 \qquad (19)$$

$$2Ru(bpy)_3^{3+} + H_2O_2 \rightarrow 2Ru(bpy)_3^{2+} + O_2 + 2H^+ \qquad (21)$$

**SCHEME 3**

$$*Ru(bpy)_3^{2+} + O_2 \rightarrow [Ru(bpy)_3^{2+}\cdots O_2]^* \rightarrow Ru(bpy)_3^{2+} + O_2 \qquad (23)$$

**SCHEME 4**

$$*Ru(bpy)_3^{2+} + O_2 \rightarrow Ru(bpy)_3^{2+} + {}^1O_2 \qquad (24)$$

The observed range of $\phi$ ($\phi = 0.25-0.28$) for $Ru(bpy)_3^{3+}$ formation from $4 \times 10^{-5}$ M $Ru(bpy)_3^{2+}$ in 9 M $H_2SO_4$ matches closely with the value of $\phi$ for luminescence quenching (Figure 6). This implies that electron transfer quenching is the dominant pathway and Schemes 3 and 4 above are relatively unimportant in this case.[23] Moreover, the close match of the quantum yields points to Scheme 1 over Scheme 2. The dominance of electron-transfer quenching is an important contributing factor to the higher degree of transient bleaching shown in Figure 9, despite the much lower luminescence quenching in 9 M $H_2SO_4$ (Table 1). Rapid charge recombination (eq 16) could be yet another factor behind the lower efficiencies at lower acidities although experimental evidence of this could not be obtained. That the irreversible absorbance bleaching in the time scale of the

**TABLE 3: Effect of the Concentrations of $H_2O_2$ and $O_2$ on the Extent of the Reverse Dark Reaction and Computation of Molar Equilibrium Constant for Equation 25**[a]

| $H_2SO_4$ | | | | | | | | |
|---|---|---|---|---|---|---|---|---|
| $\rho$, g mL$^{-1}$ | M | $m$ | $H^+$, eq M | Ru(III), eq M | Ru(II), eq M | $H_2O_2$, eq M | $O_2$, eq M | $[K_c]_u$[b] |
| 1.53 | 9 | 13.89 | 9 | $0.80 \times 10^{-5}$ | $1.20 \times 10^{-5}$ | $16.8 \times 10^{-5}$ | $29.4 \times 10^{-5}$ | $3.14 \times 10^{-3}$ |
| 1.53 | 9 | 13.89 | 9 | $0.64 \times 10^{-5}$ | $1.36 \times 10^{-5}$ | $23.3 \times 10^{-5}$ | $29.3 \times 10^{-5}$ | $2.17 \times 10^{-3}$ |
| 1.53 | 9 | 13.89 | 9 | $1.02 \times 10^{-5}$ | $0.98 \times 10^{-5}$ | $7.76 \times 10^{-5}$ | $29.5 \times 10^{-5}$ | $3.52 \times 10^{-3}$ |
| 1.53 | 9 | 13.89 | 9 | $1.08 \times 10^{-5}$ | $0.92 \times 10^{-5}$ | $7.79 \times 10^{-5}$ | $139.5 \times 10^{-5}$ | $0.95 \times 10^{-3}$ |

[a] See Table 2 for experimental details and notations. [b] $[K_c]_u$ is the uncorrected molar equilibrium constant which was computed as in Table 2 using hydrogen ion concentration instead of activity.

**TABLE 4: Redox Potentials of Tris(polypyridyl)-Ru(II) Complexes and Ferrocenium Ion from Cyclic Voltammetric Measurements at Different Acid ($H_2SO_4$) Concentrations**[a]

| | $E°$, V (vs Ag/AgCl) | | | |
|---|---|---|---|---|
| $[H_2SO_4]$, M | 1[b] | 2[c] | 3[d] | $Fc/Fc^+$ |
| 1 | 1.06 | 1.09 | 1.11 | 0.12 |
| 3 | 0.99 | 0.98 | | |
| 5 | 0.90 | 0.89 | | |
| 7 | 0.83 | 0.80 | | |
| 9 | 0.78 | 0.74 | 0.91 | −0.17 |
| 13.5 | | | 0.76 | |

[a] Scan rate = 100 mV s$^{-1}$. [b] 1 = $Ru(bpy)_3Cl_2$. [c] 2 = $Ru(phen)_3Cl_2$. [d] 3 = $Ru(bpy)_2$[4,4′-dicarboxy-2,2′-bpy]$(ClO_4)_2$.

experiments of Figures 8 and 9 is due to photooxidation is conclusively established from the concomitant rise in the absorbance at 650 nm, which persists well after complete decay of the excited-state luminescence. This can be ascribed to $Ru(bpy)_3^{3+}$ formation only. Calculations based on Figure 8, which take into account the relative molar extinction coefficient values [$\epsilon_{395}(Ru(bpy)_3^{2+}) = 5.98 \times 10^3$ M$^{-1}$ cm$^{-1}$; $\epsilon_{650}(Ru(bpy)_3^{3+}) = 5.26 \times 10^2$ M$^{-1}$ cm$^{-1}$] and the radiation dose, yield a good fit between the loss of $Ru(bpy)_3^{2+}$, as estimated from the data at 395 nm, and formation of $Ru(bpy)_3^{3+}$. Hence oxidation of Ru(II) to Ru(III) must be occurring only via $*Ru(bpy)_3^{2+}$ and Scheme 2 is probably inoperative. These results are consistent with the qualitative observation that the quantum yield does not increase at higher concentrations of Ru(II); indeed, it decreases possibly on account of self-quenching. When a pinch of $KO_2$ is added to 9 M $H_2SO_4$, instant effervescence is observed, presumably due to generation of oxygen gas via the mechanism of eq 20. The facile nature of this process below pH 4.5 ($k = 8.6 \times 10^5$ M$^{-1}$ s$^{-1}$) has been reported previously by others.[33] These results strongly suggest that $H_2O_2$ is formed in the present study through eq 20 and the pathway of eq 18 is unlikely although such a mechanism has been proposed for $H_2O_2$ formation in the riboflavin system.[34] It is noteworthy that the $HO_2^•$ intermediate does not degrade the ruthenium complex to any measurable extent;[12] instead, it stays around long enough until it finds a partner for eq 20. Disproportionation reactions are a useful means of circumventing multielectron-transfer processes as would otherwise be necessary for $H_2O_2$ formation.[2f,34]

The remaining question is, what leads to facile formation of $HO_2^•$ in high acid? First, $O_2^{•-}$ must be formed in preference to $O_2$ ($^1\Delta_g$) whereas calculations of the free energies at pH 7 suggest otherwise.[3,16] A shift in the reduction potential of the $O_2/O_2^{•-}$ couple (>0.45 V shift is necessary) in the highly acidic environment is therefore likely.[35] Such a shift could arise from weak interaction of $O_2$ with $H^+$, which would make the dioxygen molecule a better oxidant, although this might reasonably be expected to have some effect on the solubility of the gas which is not observed. In situ formation of $HO_2^•$ via the above process would also be the most efficient mechanism of warding off possible nucleophilic attack on the bipyridyl ring and suppressing the back electron donation (eq 16) which otherwise would have been inevitable. Alternatively, the $O_2^{•-}$ transient species must be trapped rapidly. Our calculations provide evidence of adequate mobility of $H^+$ within the lifetime of the excited state even when the $H_2SO_4$ concentration is as low as 0.1 M.[36] Similar trapping by protons has also been proposed by Zhang et al.[23] However, trapping of $O_2^{•-}$ by protons is not an adequate explanation since, as mentioned above, such trapping is possible even in 0.1 M $H_2SO_4$, whereas the generation of charge-separated species in significant amounts is not observed experimentally. The high ionic strength and changes in the overall thermodynamics of the system at high acid concentration must also, in some way, influence the recombination process.

**Reverse Dark Reaction.** Although the photobleaching of $Ru(bpy)_3^{2+}$ appears irreversible in the transient studies up to 160 $\mu$s, the oxidized complex reverts partially to $Ru(bpy)_3^{2+}$ when stored in dark, even in 7−9 M $H_2SO_4$. The rate and extent of reduction both increase with decreasing acidity. Since studies with electrooxidized $Ru(bpy)_3^{3+}$ reveal that the reduction caused by the medium alone is negligible in the time frame of interest, the observed dark reaction with photooxidized solution must be on account of $H_2O_2$.[37] Upon addition of 1 equiv of $H_2O_2$ into the electrochemically produced $Ru(bpy)_3^{3+}$ solution, the results of the photochemically oxidized solution are reproduced. Besides confirming the role of $H_2O_2$ as the reductant in the dark process, this study corroborates the GC evidence of near-stoichiometric $H_2O_2$ formation in the photochemical process (Figure 5). The observation that complete photooxidation of $Ru(bpy)_3^{2+}$ becomes increasingly difficult after 10 turnover numbers in 9 M $H_2SO_4$, even though there is no apparent degradation of the complex, can also be rationalized in terms of gradual buildup of $H_2O_2$, which, in turn, promotes the reverse dark reaction (Table 3). The reverse reaction might also partly explain the less than stoichiometric formation of $H_2O_2$ shown in Figure 5.

Previous work by Creutz and Sutin had established that the reaction of $Ru(bpy)_3^{3+}$ with $H_2O_2$ proceeds spontaneously in the pH range 0−10, yielding $Ru(bpy)_3^{2+}$ and $O_2$ as the main reaction products (eq 21). The reaction was found to be first order with $k = 2.7 \times 10^7$ and 4.2 M$^{-1}$ s$^{-1}$ for the $HO_2^-$ and $H_2O_2$ species, respectively.[11] This is consistent with the observed decrease in the speed of the reverse reaction with increasing acidity. The reaction also becomes less favorable (Figure 10). There is a close resemblance between the plots of Figures 2 (insert) and 10 even though these were approached from opposite directions. We infer that the forward and reverse processes are broadly controlled by the equilibrium of eq 25.

$$2Ru(bpy)_3^{2+} + O_2 + 2H^+ \underset{\text{dark}}{\overset{h\nu}{\rightleftharpoons}} 2Ru(bpy)_3^{3+} + H_2O_2 \quad (25)$$

The role of light in the forward process is presumably to overcome the activation barrier since the reaction fails to proceed

at all in the absence of light even though partial oxidation might have been expected thermodynamically. Light drives the reaction uphill as well since, in all cases, the extent of photooxidation under steady-state photolysis in sunlight (inset of Figure 2) exceeds the Ru(III) remaining in the reverse dark process (Figure 10). This is facilitated by the rate difference between the forward and reverse reactions, the latter being much slower at all acid concentrations studied. To the extent that the photooxidation is driven past the equilibrium, there is uphill conversion of light energy into chemical energy. Values of $K_c$ (based on molar concentrations) for eq 25 were evaluated for each of the acid concentrations studied (Table 2).[38] $H^+$ and $HSO_4^-$ are assumed to be the dominant forms of $H_2SO_4$ in the concentration range (1−9 M) studied since p$K$ for the second dissociation constant is 1.99,[39a] while specific conductance data suggests that the first dissociation is suppressed only at concentrations beyond 90 wt % of acid.[39b] Oxygen concentrations of the initial aerated solutions were computed from Henry's law and the concentration of 1.28 mM for $[O_2]_{sat}$ obtained from luminescence quenching measurements (vide supra), whereas values at equilibrium were computed assuming eq 25. Values of proton activity coefficient, $[\gamma_{H^+}]_m$, for the molality function were obtained from a plot of the available literature data on unscaled Pitzer single ion activity coefficient (Supporting Information; Figure 4),[40] and converted into the molarity scale ($[\gamma_{H^+}]_M$) using eq 26, which is obtained by application of the classical equations to the present system, where $H^+$, $HSO_4^-$, and $H_2O$ are the principal components; $\rho_{ov}$ and $\rho$ are the densities of the solvent

$$[\gamma_{H^+}]_M = [\gamma_{H^+}]_m \rho_{ov}[1 + 98m/1000]/\rho \qquad (26)$$

(water in the present case) and solution, respectively.[38,41] As no data on proton activity coefficient is available at 9 M (13.89 m) $H_2SO_4$, it was not possible to compute $K_c$ incorporating hydrogen ion activity. For the remaining concentrations, the values of $K_c$ are comparable with the exception of the data for 7 M acid. The variation could be on account of factors such as: nonattainment of true equilibrium and inaccuracies in values of proton activity coefficient used. As can be seen from Figure 4 [Supporting Information], $[\gamma_{H^+}]_m$ increases very steeply with acid concentration and, therefore, substantial errors in the higher range of acid concentrations are likely which would affect $K_c$ very significantly. For example, if a $[\gamma_{H^+}]_M$ value of 14.00 is used for the computation of $K_c$ at 7 M $H_2SO_4$, the value of $K_c$ would be 1.33 instead of the value of 0.39 shown in Table 2. The former is comparable to the values in 2−5 M acid. $K_c$ was also calculated at two different concentrations of $H_2O_2$ and $O_2$ (Table 3). However, since these studies were conducted in 9 M $H_2SO_4$, for which the value of $[\gamma_{H^+}]_m$ is not available, hydrogen ion concentration was used—instead of hydrogen ion activity—for the computation of $K_c$. The values were similar in the former case but rather dissimilar in the latter case even though some inhibitory effect of $O_2$ on the reverse dark reaction is evident from the spectral studies conducted. The results and discussions above reveal that eq 25 is delicately balanced, with the equilibrium shifting from left to right in the vicinity of 3−5 M $H_2SO_4$, largely on account of steep changes in $\gamma_{H+}$. Since the reduction potential of $Ru(bpy)_3^{3+/2+}$ does not actually shift despite the apparent changes observed (Figure 3), it is likely that changes in $E(O_2/H_2O_2)$ [$E° = 0.281$ V vs NHE at pH 7] brought about by the steep changes in $\gamma_{H^+}$, which, in turn, can lead to large negative pH values with increasing acid strength,[40] are responsible for the observed effects. A 59 mV/pH shift is expected on the basis of Nernst equation [$E° = (0.059/n)\log K$ at 25 °C],[42] and pH can decrease dramatically to large negative values beyond 5 M $H_2SO_4$, especially if the MacInnes convention for scaling Pitzer single-ion activity coefficients is used.[43] Decreases in the potentials of $O_2/O_2^{\bullet-}$ and $O_2/H_2O_2$ with increasing acid strength would help suppress energy transfer quenching besides promoting the overall thermodynamics of the process. Direct measurement of these potential shifts would be of considerable interest.

## Conclusions

The photooxidation efficiency of $Ru(bpy)_3^{2+}$ in oxygenated aqueous solutions shows a marked dependence on acid concentration and, for experiments with $H_2SO_4$, a sharp change is observed in the region of 2−7 M acid. Oxidation to $Ru(bpy)_3^{3+}$ is quantitative in 7−9 M $H_2SO_4$, with $H_2O_2$ formed as reduced product in near-stoichiometric yield. The high quantum yield and selectivity of the reaction may be ascribed to (i) predominance of the electron transfer quenching pathway over all others and (ii) highly efficient trapping of $O_2^{\bullet-}$ by $H^+$ followed by rapid disproportionation to $H_2O_2$ and $O_2$. These are likely on account of the high ionic strength and proton activity coefficient which favor the required shifts in the potentials of the $O_2/O_2^{\bullet-}$ and $O_2/H_2O_2$ couples. Although the above reaction is irreversible within the time scale of transient measurements, it is partly reversible in the dark over a longer duration. The equilibrium of eq 25 lies to the right for $[H_2SO_4] \geq 7$ M. Since spectroscopic evidence negates the possibility of a true shift in the redox potential of $Ru(bpy)_3^{3+/2+}$, $H_2O_2$ is presumed to be highly stabilized in strong acid medium and, therefore, less capable of reducing $Ru(bpy)_3^{3+}$ unlike at higher pH. Even though a measurable extent of spontaneous oxidation would be expected from the thermodynamic results reported herein, there is no observable change in the dark. Light helps overcome the activation barrier of the forward reaction by driving it via $*Ru(bpy)_3^{2+}$. To the extent that the photooxidation is driven past the equilibrium, there is conversion of light energy in the form of long-lived chemical products. These results are encouraging considering the simplicity with which $H_2O_2$ can be generated, the clean transformation achieved, and the high quantum yield realized.

**Acknowledgment.** P.K.G. is indebted to Dr Norman Sutin for his valuable suggestions and comments and acknowledges the assistance received from members of the Analytical section of ICI India Research & Technology Center. The authors also thank the referees for helpful comments and suggestions. The support of ICI India Limited, Council of Scientific & Industrial Research, India, and Office of Basic Energy Science of the U.S. Department of Energy is gratefully acknowledged. This is contribution No. NDRL 4247 from Notre Dame Radiation Laboratory.

**Supporting Information Available:** Various analytical data, spectra of $Ru(bpy)_3^{2+}$ in solutions of $H_2SO_4$ and plot of $\gamma_{H^+}$ vs molal concentration of $H_2SO_4$ (four figures). This material is available free of charge via the Internet at http://pubs.acs.org.

## References and Notes

(1) (a) Inada, T. N.; Miyazawa, C. S.; Kikuchi, K.; Yamauchi, M.; Nagata, T.; Takahashi, Y.; Ikeda, H.; Miyashi, T. *J. Am. Chem. Soc.* **1999**, *121*, 7211. (b) Hong, B.; Ortega, J. V. *Angew. Chem., Int. Ed. Engl.* **1998**, *37*, 2131. (c) Seroni, P.; Paolucci, F.; Paradisi, C.; Juris, A.; Roffia, S.; Seroni, S.; Campagna, S.; Bard, A. J. *J. Am. Chem. Soc.* **1998**, *120*, 5480. (d) Ramamurthy, V.; Lakshminarashimhan, P.; Grey, C. P.; Johnston, L. J. *Chem. Commun.* **1998**, 2411. (e) Maggini, M.; Guldi, D. M.; Mondini, S.; Scorrano, G.; Paolucci, F.; Ceroni, P.; Roffia, S. *Chem. Eur. J.* **1998**, *4*, 1992. (f) Andersson, M.; Linke, M.; Chambron, J.-C.; Davidsson, J.; Heitz,

V.; Sauvage, J.-P.; Hammarstrom, L. *J. Am. Chem. Soc.* **2000**, *122*, 3526. (g) Zadykowicz, J.; Potvin, P. G. *Inorg. Chem.* **1999**, *38*, 2434. (h) Indelli, M. T.; Scandola, F.; Flamigni, L.; Collin, J. P.; Sauvage, J.-P.; Sour, A. *Inorg. Chem.* **1997**, *36*, 4247. (i) Lehn, J.-M. *Supramolecular Chemistry: Concepts and Perspectives*; VCH: Weinheim, 1995. (j) Kiwi, J.; Grätzel, M. *J. Am. Chem. Soc.* **1979**, *101*, 7214. (k) Hagfeldt, A.; Grätzel, M. *Acc. Chem. Res.* **2000**, *33*, 269.

(2) (a) Morales, I.; La Rosa, D. *Sol. Energy* **1992**, *49*, 41. (b) Hee, L. T. S.; Jacquet, L.; Meshmaker, A. K. D. *J. Photochem. Photobiol., A* **1994**, *81*, 169. (c) Fujishima, A.; Honda, K. *Nature* **1972**, *238*, 37. (d) Renneke, R. F.; Hill, C. L. *Angew. Chem., Int. Ed. Engl.* **1988**, *27*, 1526. (e) Das, S. K.; Dutta, P. K. *Microporous Mesoporous Mater.* **1998**, *22*, 475. (f) Peterson, M. W.; Rivers, D. S.; Richman, R. M. *J. Am. Chem. Soc.* **1985**, *107*, 2907.

(3) Juris, F.; Balzani, V.; Barigelletti, F.; Campagna, S.; Belser, P.; Zelewsky, A. V. *Coord. Chem. Rev.* **1988**, *84*, 85.

(4) (a) Weller, A. In *Supramolecular Photochemistry*; Balzani, V., Ed.; NATO ASI Series 214, P-343; Reidel: Dordrecht, 1987. (b) Balzani, V., Scandola, F., Eds. *Supramoleculr Photochemistry*; Ellis Horwood Ltd.: Chichester, U.K., 1991.

(5) (a) Sykora, M.; Kincaid, J. R. *Nature* **1997**, *387*, 162. (b) Ziessel, R.; Hissler, M.; El-ghayoury, A.; Harriman, A. *Coord. Chem. Rev.* **1998**, *178*−*80*, 1251. (c) Ross, H. B.; Boldaji, M.; Rillema, D. P.; Blanton, C. B.; White, R. P. *Inorg. Chem.* **1989**, *28*, 1013. (d) Strouse, G. F.; Anderson, P. A.; Schoonover, J. R.; Meyer, T. J.; Keene, F. R. *Inorg. Chem.* **1992**, *31*, 3004. (e) Balzani, V.; Juris, A.; Venturi, M.; Campagna, S.; Serroni, S. *Chem. Rev.* **1996**, *96*, 759. (f) Keene, F. R. *Coord. Chem. Rev.* **1997**, *166*, 121. (g) Connors, P. J., Jr.; Tzalis, D.; Dunnick, A. L.; Tor, Y. *Inorg. Chem*, **1998**, *37*, 1121.

(6) Willner, I.; Otvos, J. W.; Calvin, M. *J. Am. Chem. Soc.* **1981**, *103*, 3203.

(7) Kalyansundaram, K., Ed. *Photochemistry of Polypyridyl and Porphyrin Complexes*; Academic Press: London, U.K., 1992.

(8) (a) Grätzel, M. In *Micellization and Microemulsion*; Mittal, K. L., Ed.; Plenum Press: New York, 1977; Vol. 2, p 531. (b) *:* Lehn, J.-M., Connoly, J. S., Eds. *Photochemical Conversion and Storage of Solar Energy;* Academic Press: New York, 1981, P-131. (c) Thomas, J. K. *Chem. Rev.* **1980**, *80*, 283.

(9) Lehn, J.-M.; Sauvage, J. P.; Ziessel, R. *Nouv, J. Chim.* **1980**, *4*, 81.

(10) Harriman, A., West M. A., Eds.; *Photogeneration of Hydrogen*; Academic Press: London, 1982.

(11) Creutz, C.; Sutin, N. *Proc. Nat. Acad. Sci. U. S. A.* **1975**, *72*, 2858.

(12) Ghosh, P. K.; Brunschwig, B. S.; Chou, M.; Creutz, C.; Sutin, N. *J. Am. Chem. Soc.* **1984**, *106*, 4772.

(13) (a) Ya Shafirovich, V.; Strelets, V. V. *Nouv. J. Chim.* **1978**, *2*, 1999. (b) Brunschwig, B. S.; Chou, M.; Creutz, C.; Ghosh, P. K.; Sutin, N. *J. Am. Chem. Soc.* **1983**, *105*, 4832.

(14) (a) Blondeel, G.; Harriman, A.; Porter, G.; Urwin, D.; Kiwi, J. *J. Phys. Chem.* **1983**, *87*, 2629. (b) Mills, A.; Lawrence, C.; Enos, R. *Chem. Commun.* **1984**, 1436.

(15) Calvin, M. *Acc. Chem. Res.* **1978**, *11*, 369.

(16) (a) Wilkinson, F.; Helman, W. P. *J. Phys. Chem. Ref. Data* **1993**, *22*, 113 and references therein. (b) Zahir, K. O.; Haim, A. *J. Photochem. Photobiol. A* **1992**, *63*, 167. (c) $E°(^1\Delta_g/^3\Delta) = 0.98$ eV and $E°(O_2/O_2^{\bullet-}) = -0.16$V and $\Delta G°(CT) = -E_{oo} + e\,[E°(Ru(III)/Ru(II)) - E°(O_2/O_2^{\bullet-})]$. (d) Miller, S. S.; Zahir, K.; Haim, A. *Inorg. Chem.* **1985**, *24*, 3978. (e) See footnote 26 in Lin, C.-T.; Sutin, N. *J. Phys. Chem.* **1976**, *80*, 97.

(17) Winterle, J. S.; Kliger, D. S.; Hammond, G. S. *J. Am. Chem. Soc.* **1976**, *98*, 3719.

(18) (a) Mulazzani, Q. G.; Ciano, M.; D'Angelantonio, M.; Venturi, M.; Rodgers, M. A. J. *J. Am. Chem. Soc.* **1988**, *110*, 2451. (b) Venturi, M.; Mulazzani, Q. G.; Hoffman, M. Z. *J. Phys. Chem.* **1984**, 88, 912.

(19) Joshi, V.; Ghosh, P. K. *J. Am. Chem. Soc*. **1989**, *111*, 5604.

(20) Kotkar, D.; Ghosh, P. K. *Inorg. Chem.* **1987**, *26*, 208.

(21) (a) Joshi, V.; Kotkar, D.; Ghosh, P. K. *J. Am. Chem. Soc*. **1986**, *108*, 4650. (b) Joshi, V.; Ghosh, P. K. *Chem. Commun.* **1987**, 789.

(22) (a) Ghosh, P. K.; Joshi, V. Indian Patent 164358, 1989. (b) Kotkar, D.; Joshi, V.; Ghosh, P. K. *Chem. Commun.* **1987**, 4.

(23) Zhang, X.; Rodgers, M. A. J. *J. Phys. Chem.* **1995**, *99*, 12797.

(24) Young, R. C.; Meyer, T. J.; Whitten, D. G. *J. Am. Chem. Soc.* **1976**, *98*, 286.

(25) (a) Nagarajan, V.; Fessenden, R. W. *J. Phys. Chem.* **1985**, *89*, 2330. (b) Kamat, P. V.; Gopidas, K. R.; Mukherjee, T.; Joshi, V.; Kotkar, D.; Pathak V. S.; Ghosh, P. K. *J. Phys. Chem.* **1991**, *95*, 10009. (c) Thomas, M. D.; Hug, G. L. *Comput. Chem.* **1998**, *22*, 491.

(26) Optical rotation value for freshly prepared solution of (−)Ru(bpy)$_3$Br$_2$·6H$_2$O ($5.0 \times 10^{-4}$M) in 9M sulfuric acid solution was 0.45, while that for a solution stored in dark for 7 days was −0.44.

(27) After five complete cycles of photochemical oxidation and electrochemical reduction, elemental analyses values for the isolated ruthenium complex are C, 40.7%; H, 2.5%; N, 9.17%. The calculated values for Ru(bpy)$_3$(PF$_6$)$_2$.H$_2$O are: C, 41.0%; H, 2.95%; N, 9.76%. Corresponding optical rotation values obtained directly for the solutions containing 2 mM $\Delta(-)_D$-Ru(II)- were identical at 0.143° after five cycles, keeping measurement conditions the same.

(28) Schilt, A. A. *Anal. Chem.* **1963**, *35*, 1599.

(29) Bard, A. J.; Faulkner, L. R. *Electrochemical Methods: Fundamentals and Applications*; John Wiley & Sons Inc.: New York, 1980.

(30) Weston, R. E., Jr.; Schwarz, H. A. In *Chemical Kinetics*; Johnston, H. S., Ed.; Fundamental Topics of Physical Chemistry Series; Prentice Hall Inc., Englewood Cliffs, NJ, 1972.

(31) Turro, N. J. *Modern Molecular Photochemistry*; The Benjamin/Cummins Publishing Company Inc.: Menlo Park, CA, 1978.

(32) Atkins, P. W. *Physical Chemistry*, 3rd ed.; Oxford University Press: U. K., 1986.

(33) (a) Slama-Schwok, A.; Gershuni, S.; Rabani, J.; Cohen, H.; Meyerstein, D. *J. Phys. Chem.* **1985**, *89*, 2460. (b) Bielski, B. H. *J. Photochem. Photobiol.* **1978**, *28*, 645. (c) Fee, J. A.; Valentine, J. S. In *Superoxide and Superoxide Dismutase*; Michelsen, A. M., McCord, J. M., Fridovich, I. Eds.; Academic Press: New York, 1977. (c) Konya, K. G.; Paul, T.; Lin, S.; Lusztyk, J.; Ingold, K. U. *J. Am. Chem. Soc*. **2000**, *122*, 7518.

(34) Gallardo, F.; Galvez, S.; Medina, M. A.; Heredia, A. *J. Chem. Educ*., **2000**, *77*, 375.

(35) The $O_2/O_2^-$ couple is reportedly sensitive to the solvent media, e.g., the E° values being −0.60 V vs NHE in pyridine versus −0.16 V vs NHE in water (pH 7). The reduction potential could shift to still less negative values in acidic medium,[31] and attempts are underway to establish the magnitude of shift experimentally.

(36) With $l = (2D\tau)^{1/2}$ ($D_{acid} = D_{water}(\eta_{water}/\eta_{acid})$ where $D_{water} = 9.3 \times 10^{-5}$ cm$^2$/s) and $\tau = 0.398$ $\mu$s for *Ru(bpy)$_3^{2+}$, the diffusion length is calculated to be 50 nm in 9 M $H_2SO_4$, while one $H^+$ ion can be found in a volume space of $9.2 \times 10^{-23}$ mL, which translates to a unit cell length of 0.45 nm. The corresponding values are 60.9 nm and 2.0 nm in 0.1 M $H_2SO_4$. Thus the possibility for a proton to trap the transient $O_2^{\bullet-}$ in the activated complex is high even in the lower range of acid concentration.

(37) In contrast, Ru(bpy)$_3^{3+}$ can react with the aqueous medium at higher values of pH. In this reaction, ca. 5% of the complex molecules are oxidatively degraded (ligand degradation all the way to yield $CO_2$ was also observed) to provide the electrons necessary to reduce the remaining 95% of molecules.[12] On the other hand, $O_2$ could be generated in the presence of $Co^{2+}$ and $RuO_2$ as catalysts.[3,13−15]

(38) The equilibrium constant can also be expressed in terms of mole fraction: $K_x = K_c(\Sigma M_i)^{-\Delta\nu}$, where $\Delta\nu = -2$ for eq 25 and $M_i$'s are the molar concentrations of the various chemical species (Castellan, G. W. *Physical Chemistry*; Addison-Wesley Publishing Company: Reading, U.K., 1970).

(39) (a) Lide, D. R., Ed. *Handbook of Chemistry and Physics*, 79th ed.; CRC Press: Boca Raton, FL, 1998. (b) *Kirk-Othmer Encyclopedia of Chemical Technology*, 3rd ed.; Wiley-Interscience: New York, 1983; Vol. 22, p 195.

(40) Nordstrom, D. K.; Alpers, C. N.; Ptacek, C. J.; Blowes, G. W. *Environ. Sci. Technol.* **2000**, *34*, 254.

(41) Wall, F. T. *Chemical Thermodynamics*, 3rd ed.; W. H. Freeman & Co.: San Francisco, 1965; p 418.

(42) Sawyer, D. T., Nanni, E. J., Jr., Eds. *Oxygen and Oxy-radicals in Chemistry and Biology*; Academic Press Inc.: New York, 1981; p 15.

(43) Values computed following the MacInnes convention for scaling Pitzer single-ion activity coefficients suggest that, while $\gamma_{H^+}$ and pH are 2.12 and −0.79 in 2.3 molal $H_2SO_4$, the corresponding values are 1200 and −4.09 in 9.8 molal acid.[40] pH values could be still lower in 9 M acid (13.89 m).